

Document downloaded from:

<http://hdl.handle.net/10251/153694>

This paper must be cited as:

Reinosa, JJ.; García-Baños, B.; Catalá Civera, JM.; Fernández Lozano, JF. (2019). A step ahead on efficient microwave heating for kaolinite. *Applied Clay Science*. 168:237-243.
<https://doi.org/10.1016/j.clay.2018.11.001>



The final publication is available at

<https://doi.org/10.1016/j.clay.2018.11.001>

Copyright Elsevier

Additional Information

32 1. INTRODUCTION

33 One of the most critical issues in today's society is the large amount of greenhouse
34 gasses generated annually in thermal processes. The growing energy consumption
35 coupled with the demand for materials is in part at the origin of this excessive increase
36 in resources. Today, the society challenge is increasing the energy production from
37 renewable and non-polluting sources. Moreover, green energy production also seeks to
38 use energy in an efficient way, as an example, by electric vehicles with batteries.
39 However, industrial production of bulk materials still requires high temperature
40 treatments associated to further bearing gas emissions by decomposition of raw
41 materials. Thus, the main sectors of infrastructure and building topped the list of
42 industrialized materials of mass production as cements, ceramics or glasses. A
43 common aspect of these materials is the use of large quantity of mineral raw materials
44 that require heat treatments at high temperatures, above 1000°C. In most cases, fossil
45 fuels or gas are used for thermal processing. Generally speaking, the electric furnaces
46 are inefficient and incompatible with the processing rates of tons per hour that most of
47 these materials require. The relevant question to be answered is whether there is any
48 possibility to use electricity in an efficient way for the heat treatment of materials.

49 In this regard, the use of microwave energy is extensively proposed as an efficient
50 thermal process of materials which are capable of absorbing electromagnetic radiation
51 ([Thostenson and Chou, 1999](#)). In this case, sintering times decrease, in general the
52 processes need lower temperatures ([Roy et al., 1999](#)), and in mostly of cases “in situ”
53 CO₂ emissions are reduced in comparison with combustion processes. The lack of
54 knowledge related to the materials behaviour under microwave radiation is limiting up
55 today the heating applications to the laboratory scale. So, it is required a breakthrough
56 to open the way to use microwave technology in the mass production processing of
57 materials at high temperature.

58 In conventional heating methods the heat is transferred between objects through the
59 mechanisms of conduction, radiation and convection. In this case, the surface of the
60 material is firstly heated and then, there is a temperature gradient from the surface to
61 bulk of the material. By comparison, in microwaves heating processes, the
62 electromagnetic energy is absorbed volumetrically by the material and transforms into
63 heat. Thus, the energy could directly transfer to the material within an inner uniform
64 temperature distribution ([Oghbaei and Mirzaee, 2010](#)). Microwaves can interact with
65 materials through either polarization or conduction processes ([Sun et al., 2016](#)). Both
66 processes give rise to dielectric losses at certain frequency ranges. The dielectric
67 losses are due to ion conduction at lower frequencies and to rotation of permanent
68 dipoles at higher frequencies. Thus the dielectric properties ultimately determine the
69 effect of the electromagnetic field on the material. Overall, there are three types of
70 materials according to the response to the microwave radiation: reflector, receptive,
71 and transparent. Materials with high conductance and low capacitance, such as metals,
72 have high dielectric loss factors. As the dielectric loss factor gets very large values, the
73 penetration depth of microwaves approaches zero and the materials are considered as
74 microwave reflectors or mirrors. Conversely, in materials with low dielectric loss factors
75 very little amount of electromagnetic energy interacts with the material and it is
76 considered as transparent material against microwave energy ([Mandal and Sen, 2017](#)).
77 Microwave radiation transfers energy most effectively to materials that have
78 semiconductor behaviour and medium dielectric loss factors. In contrast, conventional
79 heating transfers heat in a most efficiently way to materials with high thermal
80 conductivity ([Oghbaei and Mirzaee, 2010](#)).

81 The potential use of heating by microwave energy inspires to the materials towards the
82 efficient use of energy. The reason is that there are challenging demands from the
83 industry for new and improved thermal processes in order to obtain finer
84 microstructures and to enhance physical and chemical properties, apart from the
85 mentioned advantages of the use of microwaves energy ([Leonelli et al., 2008](#)). In this

86 sense, many experiments were performed applying microwaves energy at laboratory
87 scale ([García-Baños et al., 2016](#)) by using 2.45GHz as frequency band because it is
88 the standard magnetron frequency for domestic microwaves. But in general, at room
89 temperature oxide materials do not absorb microwaves appreciably at 2.45 GHz. In
90 order to improve microwave absorption by the oxides, several attempts were pursuit
91 as: conventional preheating; by adding absorbents (e.g., SiC, carbon, binders)
92 ([Bhattacharya and Basak, 2017](#)); by altering the materials microstructure and the
93 defects structure as [Agrawal \(1998\)](#); by changing their form (e.g., bulk vs. powder); or
94 by tuning the frequency ([Clark and Sutton, 1996](#)). In this way, the behavior of some
95 ceramic oxides which are widely used in different application fields as Al₂O₃, TiO₂, ZnO
96 and Bi₂O₃ were studied versus microwaves interaction ([Bindra and S. Bahel, 2010](#)).
97 Also advanced materials as PZT, BaTiO₃, ceramic perovskites or ZnO varistors were
98 thermally processed by using microwaves energy. ([Clark et al., 2005](#); [Fang et al., 2009](#))
99 In these experiments the “microwave effect” is claimed to be behind a faster thermal
100 treatment. The “microwaves effect” is described as a non-thermal phenomenon that
101 consists of accelerated kinetics ([Vaidhyanathan et al., 2001](#); [Roy et al., 2002](#)). In a
102 sintering process, the microwave effect is quantified by the difference between the
103 required temperatures by microwave heating versus conventional heating, typically
104 electrical heating, that leads similar microstructures. In this sense, saving in energy
105 consumptions is argued thanks to microwaves energy application.

106 Nowadays a large volume of non-metallic mineral products in industry is manufactured
107 by thermal processes. Non-metallic mineral industry is dominated by cement, glass and
108 ceramic industries. Large amounts of energy are used in heating processes at high
109 temperatures of non-metallic minerals which inevitably produce large quantities of
110 greenhouse gasses, mainly CO₂. A clear example is the cement industries which are
111 responsible for ca. 10% of CO₂ world production from carbonate oxidation and fuel
112 combustion ([Olivier et al., 2014](#)). But non-metallic minerals are transparent to the

113 microwave radiation. However, the challenge to use microwave energy in the heating
114 processes could make possible to drastically reduce the amount of CO₂ from fossil
115 fuels. Moreover, the lack of knowledge related to the behavior of non-metallic minerals
116 under microwave radiation versus temperature impedes to realize the transformation of
117 these industries. One clay mineral that is present in most of the cement, glass and
118 ceramic production processes are kaolinite. Kaolinite is part of the group of industrial
119 minerals, with the chemical composition Al₂Si₂O₅(OH)₄. It is a layered clay mineral, as
120 for such, the individual layers consist of tetrahedral layers of silica (SiO₄) linked through
121 oxygen atoms to octahedral layers of alumina (AlO₆). Rocks rich in kaolinite are known
122 as well as fire kaolin clay or ball clay. Brindley and Nakahira, 1959 reported the
123 reaction series from Kaolinite-mullite during the thermal treatment in a conventional
124 heating.

125 In this sense, this work shows an in situ study of the dielectric properties of kaolin clay
126 under microwaves radiation. The thermal behaviour of kaolin is compared with the
127 observed by conventional heating. Therefore, dielectric properties are studied and
128 microwave effect for large heating rates at temperatures >650°C is correlated with the
129 drastic drop of resistivity in the kaolinite after the dehydroxylation process. A
130 mechanism for effective heating under microwaves radiation is proposed based on the
131 electron-phonon-coupling. The study is a first step in the knowledge of the application
132 of microwaves with the purpose of heating large amounts of materials that generate
133 high CO₂ emissions during heating, such as kaolinite-based materials as kaolin clay.

134 2. EXPERIMENTAL PROCEDURE

135 Pure industrial-type kaolin clay (from Keraben Group, reference MK_KE01) having
136 96% of kaolinite was chosen for the study. The kaolin clay raw material in form of
137 powder was sieved using a mesh of 100µm and die pressed at 25MPa to obtain
138 cylindrical samples with dimensions of 1mm (for electrical resistance and impedance

139 measures) or 10 mm (for dielectric assays by applying microwaves energy) in
140 thickness and 10 mm in diameter. Samples were thermally treated at different heating
141 rates (from 5 to 40°C/min) up to 1100°C by using two different heating methodologies:
142 - Conventional: electrical furnace Nabertherm Model L9 from Germany with a program
143 controller S27.
144 - Microwaves: microwaves laboratory equipment where the microwave cell is a
145 cylindrical resonance cavity designed to operate simultaneously in two modes, one for
146 heating and the other one for measuring, as [Catalá-Civera et al. 2015](#) designed. The
147 heating mode (TE₁₁₁), designed to resonate near the ISM standard frequency of 2.45
148 GHz, is fed into the cavity by a probe inserted through the side wall ([Figure S1](#)). Once
149 tube and sample are positioned inside the cavity, control software implemented in
150 Labview allows setting the desired heating rate, monitoring the sample temperature,
151 recording the video image of the sample and the response of the cavity, both for the
152 measuring and heating modes. A PID algorithm adjusts the source bandwidth to follow
153 the changes in the cavity response and obtain the desired heating rate throughout the
154 process.

155 The samples were characterized chemically by X-ray fluorescence using a XRF Philips
156 MagiX spectrometer, structurally by X-ray diffraction using a Bruker AXS D8 – Advance
157 diffractometer (Madison, WI, USA.), granulometrically by laser diffraction using a
158 Malvern Mastersize equipment, and microstructurally by using a Field Emission
159 Scanning Electronic Microscope FESEM Hitachi S-4700, Hitachi. The thermal
160 transformations in the range 30–1200 °C with a heating rate of 10°C/min were studied
161 by means of differential thermal, DTA, and thermogravimetric, TG, analysis using a
162 Thermo-Analizer Netzch STA 409 with a temperature controller Netzch TASC 414/2
163 being the reference α -Al₂O₃ and a Hot-stage microscopy by a Leica Leitz microscope.

164 The dielectric properties during the heating under microwave radiation were evaluated
165 in the microwaves energy laboratory equipment. The dielectric measure mode (TM₀₁₀)

166 is fed by a probe (a different one from the heating mode) through the bottom wall of the
167 cavity. A Vector Network Analyzer is used as a source for the measuring mode, with a
168 cross-coupling filter to avoid interferences between the heating and the measuring
169 signals.

170 Impedance spectroscopy allowed calculating the electrical resistance and capacitance
171 against the frequency by adequate electrical circuit's analysis. The measurements
172 were obtained by using an impedance analyzer (HP4294A, Agilent Technologies Inc.,
173 Santa Clara, CA). The frequency range was from 100Hz to 10MHz for dielectric
174 constant measurements. The temperature range is up to 700°C using a 2°C/min
175 heating-cooling rate, for both impedance measurements and for electric modulus.
176 Impedance arcs were obtained by Nyquist plot from 630°C to 700°C due to the
177 resolution of the measurements and for this reason only impedance arcs in this range
178 appear plotted. Capacitance was calculated from the value $\omega_{\max} \cdot R \cdot C = 1$, where
179 $\omega_{\max} = 2\pi f_{\max}$ and f_{\max} is the frequency at the maximum value of the impedance arc for
180 different temperatures. DC electrical resistance was measured by the same impedance
181 analyzer from 30°C to 700°C and it was recorder during heating and cooling of fresh
182 and thermally treated kaolin clay pressed discs previously electroded by using silver
183 paste.

184

185 **3. RESULTS AND DISCUSSION**

186 The behaviour of kaolin clay cylinders when they are heated by using microwave
187 energy at different constant heating rates (5 - 40°C/min) was studied ([Figure 1a](#)). In all
188 cases, at low temperatures, <650°C, kaolin clay samples heat accordingly to the
189 selected heating rate, denoted as region 1. Unexpectedly, there is a sudden increase
190 of the heating rate at ≈650°C independently of the initial selected heating rate, region 2.

191 At slower heating rates the anomalous increase of temperature is more visible in [Figure](#)
192 [1a](#). At higher temperatures the samples regulate the heating rate up to the initial
193 heating ratio, region **3**, which is more clearly observed for the lower heating rates. The
194 heating rates obtained for the different sintering cycles by using microwaves energy
195 were studied ([figure 1b](#)). The previously mentioned regions are delimited also for shake
196 of clarity. The heating rates in region 1 are in concordance with the initially selected
197 heating rates for the thermal treatments (inset in [Figure 1b](#)). Nevertheless, as it was
198 mentioned before, a change of heating ratios takes place from $\approx 650^{\circ}\text{C}$. This variation is
199 more pronounced for lower initial heating rates, it means, the anomalous experimental
200 heating rates in region 2 are inversely proportional to the ones that were programmed
201 in microwave laboratory equipment.

202 In fact, in order to keep the heating ratio constant during the initial stage of the heating
203 processes (below 200°C) by using microwaves energy, a relevant change of the
204 microwave bandwidth is required ([figure 1c](#)). At room temperature the material shows
205 low selectivity to microwave radiation and the low absorption is signalled by a higher
206 bandwidth as an indication of the low efficient heating process. At temperatures higher
207 than $\sim 160^{\circ}\text{C}$ the bandwidth decreased and this fact signalled an increase of energy
208 transferred from the microwave field to the sample. From $\sim 280^{\circ}\text{C}$, a nearly constant
209 frequency keeps the heating rate relatively constant until $\sim 650^{\circ}\text{C}$. Above 650°C the
210 bandwidth is maintained with a small increasing and a further decreasing in the region
211 **3** denotes higher absorption of microwave radiation by the sample, [figure 1c](#). The
212 enhancement of heating rates for microwave heating could be associated to the usually
213 named "microwave effect". The microwave effect thus is observed in kaolin clay
214 samples in a temperature range where the heating rate increases one order of
215 magnitude. This increase is observed for low selected heating rates. It is worth to
216 remark that, during the whole experiment, the heating source is always the microwaves
217 radiation. In this sense, region 2 shows higher efficiency in the conversion process of

218 electromagnetic radiation into heat. However, the effective heating rate could be
219 ascribing to well-known thermochemical structural changes from kaolinite to metakaolin
220 as a consequence of the temperature.

221 The main temperature points at which changes take place are correlated from
222 Differential Thermal Analysis, DTA, and Termogravimetry, TG, studies of kaolin clay
223 when it is heated conventionally (Figure 2a). At ~535°C an endothermic process that
224 corresponds to the dehydroxylation of kaolinite and then metakaolin occurs (reactions
225 are described in S2). This endothermic transformation requires energy absorption in
226 order to remove the chemically bonded hydroxyl groups. TG curve shows that nearly
227 10 wt% of water is eliminated from the structure during this reaction and therefore the
228 total mass of the kaolin clay sample decreased accordingly. The kaolinite
229 dehydroxylation is accomplished with a slight shrinkage of the sample and therefore
230 porosity usually rises in this process. Regarding the loss of water, it is worthy to
231 mention that it is a non-reversible process that provokes appearance of new defects
232 into the kaolinite structure and the material transform to metakaolin. In order to
233 understand the structural modifications, Kaolinite ($\text{Al}_2\text{O}_3 \cdot 2\text{SiO}_2 \cdot 2\text{H}_2\text{O}$) is composed by
234 a SiO_4 tetrahedrons layer and a Al_2O_3 octahedrons layer that confers the
235 characteristic laminar type morphology of clays having typically 1.24 nm in thickness
236 and more than 200 nm in equivalent diameter (Hu and Liu, 2003). The hydroxyl groups
237 are responsible for the appearance of defects on the material structure. Moreover
238 kaolinite layers are linked by hydrogen bridges between OH⁻. This morphology is the
239 responsible for the high specific surface of the kaolinite clays (Varga, 2007). The
240 structural dehydroxylation of kaolinite is produced by a combination of two different
241 processes that occur in the heating step (Sperinck et al., 2011): the continuous loss of
242 water at the inter-layer and the discontinuous loss of structural (inner-layer) water. The
243 dehydroxylation of structural water might result in the disturbance of the $\text{Al}(\text{O},\text{OH})_6$
244 octahedral layers by the outer hydroxyls, but it does not have much effect on the SiO_4

245 tetrahedral layers due to the more stable inner hydroxyls groups. The outer hydroxyls
246 of octahedral layers correspond nearly to 87% of the water in the material, and may be
247 more easily removed by heating than inner ones, that will maintain a more ordered
248 SiO₄ tetrahedral group in structure during dehydroxylation (Giesse and Datta, 1973). All
249 these processes explain the reason because the dehydroxylation process occurs in a
250 wide temperature range, from ~475 to ~583°C.

251 A further heating produces an exothermic peak at ~980°C indicating the structural re-
252 crystallization from layered units of metakaolin to aluminium-silicon spinel or pre-mullite
253 type crystals (reactions are described in figure S2) (Sahnoune et al., 2007). During this
254 process, the excess of SiO₄ tetrahedral units become amorphous silica that assists a
255 mass diffusion process and improves the densification. It is described that the
256 formation mechanism of mullite starts with two pre-reactions which consist of the
257 formation of pseudo-tetragonal mullite (at ~700°C) in a solid-liquid phase and its
258 posterior transformation to orthorhombic mullite at ~800°C as a solid state reaction.
259 (Zhang et al., 2014) These processes could explain the increase of the heating ratio
260 from 700°C in Figure 1b and the existence of variations in the band width curve of
261 Figure 1c at the mentioned temperatures.

262 It was studied the dielectric losses of kaolin as a function of the temperature under the
263 presence of microwaves radiation during heating and without microwaves radiation
264 during cooling (Figure 2b). The dielectric losses are linked to the microwaves power
265 adsorption. During heating from room temperature to ≥150°C a small decrease of the
266 dielectric losses occurs. The dielectric losses during heating remained after this
267 temperature quite below the 0.1, value that indicates low microwaves energy
268 absorption and therefore low effectiveness during heating step (Fernandez et al.,
269 2015). This fact correlates with the high values of the band width which were observed
270 for those temperatures in Figure 1c. Into the range from 475°C to 583°C, a sudden
271 increase of dielectric losses indicates a drastic change of the dielectric behaviour

272 where the loss factor exceeds the value of 1.5. This increase is un-coincident with any
273 changes in the previous microwaves heating curves, [Figure 1](#), but it is coincident with
274 the dehydroxylation process of kaolin, [Figure 2a](#). After the dielectric loss enhancement,
275 several variations of dielectric losses appear. The more intense peaks are located at
276 the temperature ranges between 800-900°C and 1090-1210°C (signalled in [figure 2b](#)).
277 This time, the effective increase of the measured heating rate is coincident with the
278 pre-reactions of the formation of pseudo-tetragonal mullite at ~700°C, its posterior
279 transformation to orthorhombic mullite at ~800°C. During cooling, none of these
280 process should occurs and, accordingly, the value of dielectric losses decreased but it
281 kept a value higher than 0.2 indicating the structural and microstructural evolution of
282 the sample. Hence, the increase of power absorption with the temperature from 650 -
283 700°C is in principle supported by the increasing of dielectric loss factor which is
284 related to the existence of amorphous silica and alumina that contributes to the mass
285 transport [for the reordering of the structure after the dehydroxylation](#).

286 The thermal conductivity of kaolinite and metakaolin keeps nearly constant in the range
287 of temperature in which both materials do not suffer changes ([Michot et al., 2008](#)). It
288 means that the changes in the dielectric behaviour of the sample during the heating
289 step have not relation to the thermal conductivity of the material. Nevertheless, the
290 densification at higher temperatures could affect the dielectric response of the sample
291 inside the resonant microwave cavity as the one used in the present work. The
292 presence of structural hydroxyl groups produces low microwave adsorption by dipole
293 rotation (as it occurs in the temperature range of 160-473°C, before the beginning of
294 the dehydroxylation process). [In addition](#) their elimination initially seems to be related
295 with the sudden improve of the heating by microwaves energy adsorption.
296 Nevertheless, a correlation between the defects originated during the dehydroxylation
297 and the sudden increase of microwaves energy absorption could be in principle
298 established. A subsequent second thermal heating on the previous sample shows a

299 similar behaviour in dielectric losses vs temperature (see [Figure S3](#)), but this time to a
300 lesser extent. During the second thermal heating the material is not able to suffer
301 dehydroxylation and thus the microwave effect that assists the higher heating rate
302 should be attributed to a different mechanism than the dipole rotation and could not be
303 related to the water elimination from the kaolin structure.

304 In order to understand the unusual behaviour of the kaolin during the dehydroxylation
305 step, an in situ measurement of the electrical resistivity was attempted in a
306 conventional furnace. The static or DC resistance of the sample was measured during
307 both the heating and the cooling steps. A drastic change in the DC resistance with the
308 increase of the temperature is found for kaolin samples ([Figure 3a](#)). The value of the
309 initial DC resistivity at room temperature, $>10^8\Omega.cm$ (not shown), is not a real value
310 because initially kaolin is an insulator compound and its resistance overflows the
311 equipment of measure ([Equipment measure range: from \$300\Omega.m\$ to \$3 \times 10^8\Omega.m\$](#)). An
312 abrupt decreasing of the DC resistivity takes place at $\sim 555^\circ C$ up to $\sim 3 \times 10^6\Omega.cm$, that it
313 is more than 2 orders of magnitude of lower resistances than the initial values. The
314 resistivity drop suffers an exponential decay. This resistance decay fits the mass losses
315 in the range of temperatures where the dehydroxylation of the kaolin takes place. It is
316 described that the mentioned decrease might arise partly for an increase in the cations
317 mobility during the dehydroxylation process ([Tari et al., 1999](#)). In this way, if the cations
318 mobility enhances, it will contribute to the total conductivity and so the resistance of the
319 entire system will decrease. It is surprisingly that the DC resistivity value recovers up to
320 $\sim 3 \times 10^8\Omega.cm$ during the cooling of the sample. Moreover, DC resistivity is recovered at
321 low temperature and the abrupt drop experiences an hysteresis, ca. $-5^\circ C$ (see inset in
322 [Figure 3a](#)). In a second heating process (at this time metakaolin is the initial compound
323 because the dehydroxylation process already took place during the first heating cycle),
324 the electrical resistivity vs temperature follows a similar trend than during the first cycle,
325 nevertheless a difference of $\sim 5^\circ C$ is also observed. This fact indicates a lack of

326 relationships between the dehydroxylation and the change of resistivity because the
327 dehydroxylation process in kaolin is not reversible. Hence, the strong drop of the
328 resistance with the temperature cannot be attributed to the water elimination. Taking
329 into account that both kaolinite and metakaolin are intrinsically resistive materials for
330 nature, the unusual changes in resistivity should be attributed to thermally activated
331 surface phenomena (Lorite et al., 2012). The presence of surface carriers are
332 originated when the OH⁻ are eliminated during heating. To remove an H₂O molecule it
333 is required two hydrogen atoms located in neighbouring hydroxyl groups, as well as
334 one of the bonded oxygen atoms from hydroxyl groups (Ondruška et al., 2015). So, the
335 remaining oxygen from hydroxyl is then converted to structural oxygen after swiping the
336 free electron located on terminal oxygen to particle edges resulting in large oscillating
337 dipoles. In other words, the vacancies which are produced by the loss of hydroxyls
338 groups from the structure create large distortion in the layers. These structural changes
339 are responsible for the appearance of surface dipoles that are thermally activated in
340 order to increase conductivity in a reversible way.

341 In order to discriminate whether a conduction mechanism takes place in the samples
342 an impedance spectroscopy analysis is attempted (Figure 3b-c). For all the heating and
343 cooling cycles the formation of a single impedance semicircle is observed at
344 temperatures >650°C (Figure S4), in the range of temperatures where the decreasing
345 of the resistivity shows an exponential decay behaviour. The impedance arcs are
346 adjusted taking into account the RC circuit described in Figure 3b inset. Typical values
347 of relaxation frequency (fr) of the impedance arc might give a good indication of the
348 nature of the main contribution to conductivity, e.g. from the intrinsic contribution as
349 crystal lattice or extrinsic contribution as grain boundaries/intergranular phases (Ribeiro
350 et al., 2004). In general, high values of relaxation frequency are ascribed to the intrinsic
351 contribution. Moreover, the values of capacity are in the order of 10⁻¹² Farads (see
352 Figure 3b) for the different temperatures and heating cycles. This aspect confirms that

353 the resistivity corresponds to the same electro-active region. The conductivity slightly
354 increases with the increasing of temperature indicating semiconductor behaviour. This
355 fact points the differences of temperature in the process of changes of resistivity
356 between the heating and the cooling step of the sample. The excitation keeps
357 remaining when temperature decreases. Due to the layered morphology of the kaolinite
358 based materials, the structural defects are present at the interfaces between the former
359 layers. Thus, the surface carriers are responsible for the increase of conductivity in
360 metakaolin and thereof behind the high heating rate observed. Zemanova et al. 2006
361 applied microwaves energy in smectite clay minerals and observed MW heating
362 efficiency thanks to an ionic conduction contribution for neutralization of layer charges.
363 In concrete, smectite presents alkali and alkali earth cations apart from electrons after
364 dehydration processes, and both charges with different polarity try to join for
365 neutralization of the system. Nevertheless, kaolinite has not alkali and earth alkaline
366 ions in the structure so the mechanism may be different. In Kaolinite, the phase change
367 at 980°C promotes the accommodation of the structure and charges so the heating
368 ration decreases after the transformation.

369 An electron-phonon-coupling mechanism could explain the microwave absorption of
370 the surface carriers to an excited state and their interaction with cations in the crystal
371 lattice, which provokes their displacement from the equilibrium positions. Electron-
372 phonon coupling is a major coherent mechanism, which often causes scattering and
373 energy dissipation in semiconductor electronic (Chen et al., 2015). In such a way the
374 microwave effect which is responsible to the observed high heating rates could be
375 ascribed to such mechanism.

376 The behaviours according to the thermal evolution of the kaolin under the presence of
377 microwaves energy and the heating mechanism of the material when is irradiated by
378 microwaves are summarized in Figure 4. At low temperature when microwaves interact
379 with kaolinite, the excitation of dipoles takes place, mostly from terminal OH. During the

380 dehydroxylation process it occurs the mechanism which consists of swiping the free
381 electron located on terminal oxygen to particle edges, resulting in large oscillating
382 dipoles induced by oscillating MW E-field. In the obtained metakaolin, the charges
383 displace along the structure because of the insulator character of the material. The
384 movement of charges along the surface causes an electron phonon-coupling, so that
385 the cations displacement in the crystal lattice from the equilibrium position is carried out
386 depending on their charge and the charge carriers. The displacements of the cations
387 promote an increase of the kinetic energy of the crystalline network since they generate
388 a quantized lattice vibration wave or phonon. The charge carriers on the surface of the
389 layered particles efficiently absorb microwave radiation. However, the sample has a
390 high resistivity, which leads to a limited density of charge carriers in it. Thus, the lack of
391 charge carriers produces inefficiency in the microwave absorption process at high
392 doses of applied energy. The same situation occurs when large heating rates are
393 programmed in the laboratory equipment. At the time that the amount of microwaves
394 energy is reduced, an increase of the efficiency occurs and thus very large efficiency is
395 obtained when the heating rate exceeds 500°C/min. In such conditions, the charge
396 carriers are excited by the microwave radiation and the electron-phonon-coupling
397 mechanism occurs. Hence, the microwaves energy is transferred into heat on the oxide
398 material. Lower heating curves than the selected ones are not attempted because of
399 the regulation instability of the laboratory equipment.

400 At higher temperatures, the presence of phonons in the crystal lattice scatters the
401 charge carrier and therefore the mobility of the charge carriers reduces considerably in
402 spite of the increase of conductivity in the material. The chemical reactions would
403 contribute also to limit the amount of charge carriers. As consequence, the electron-
404 phonon-coupling is efficient only in the range of temperature in which the surface
405 carriers are available and, in spite of the large dielectric losses, the solid reduce their
406 heating rate.

407 The implication of the above findings is quite relevant for both the academia and the
408 industry. In a first approach, the heating of minerals in mass production industries could
409 be benefited from this mechanism by combining adequate materials in order to produce
410 advanced industrial heating microwave furnaces. The authors of this publication are
411 also reporting the use of an adequate mixing of minerals to produce glass melting
412 process of frits used in the tile industry ([Daphne Project, 2012](#); [García-Baños et al.,
413 2015](#)). In this case, an adequate combination of minerals allows the efficient heating at
414 different temperatures. Temperatures higher than 1500°C are obtained and the
415 process is scaled to pilot plant production with >65% saving in terms of energy.

416 In a second approach, the selective heating of semiconductor materials, in particular
417 oxide materials having surface defects as nanomaterials, also could be benefited from
418 this effect. In this manner, higher chemical potential regions could increase rapidly their
419 temperature and surface diffusion mechanism is promoted. Additionally, electron
420 excitation between nanostructures, as quantum dots, could modulate not only the
421 electrical conductivity states in silicon quantum dots ([Ferrus et al., 2014](#)), but also the
422 thermal conductivity or local heating of the particles.

423 In summary, the presence of surface charges in semiconductors improves the heating
424 of the material by an electron-phonon coupling mechanism when microwaves energy is
425 applied. The high efficiency of the process is higher than the standard dipole rotation.

426 In this sense, the mechanism of electron-phonon-coupling could be behind the so
427 called “microwave effect” in more materials than expected because the hopping
428 mechanism appears in poor conductive materials or in high disorder materials with low
429 carrier density. The present study stimulates to find new solutions for industrial heating
430 that runs in the sense to save energy and to obtain drastic reductions of CO₂ emissions
431 when microwaves are used.

432

433 **4. CONCLUSIONS**

434 A step ahead to the effective use of microwave radiation for mass production materials
435 based on oxide minerals is shown. The dielectric properties of the kaolin samples
436 versus temperature are evaluated under microwave radiation. The thermal evolution of
437 kaolin under microwaves energy exposition shows an unexpected large heating rate up
438 to 500°C/min for temperatures >650°C. Such heating rate is associated with a
439 resistivity drop of $>10^3 \Omega.m$ observed after the kaolin dehydroxylation process and a
440 relevant increasing of the dielectric losses. While the processes of dehydroxylation of
441 the kaolin structure are not reversible, the drastic decrease in resistivity is reversible
442 with a small hysteresis and thereafter the high rate of heating which is showed under
443 microwave radiation is correlated with the charge carriers responsible for the
444 decreasing of the resistivity. The layered structure of the clay-based materials allows
445 the appearance of charge carriers at the surface after dehydroxylation and thus these
446 surface defects of the crystal lattice are electromagnetically activated. The high efficient
447 of the microwave heating effect is correlated with the presence of surface carriers that
448 absorbs microwave electromagnetic field and produces crystal heating by electron-
449 phonon-coupling or small polaron. This effect represents a breakthrough in the efficient
450 use of microwave energy in order to produce efficient thermal treatments in large
451 volume of non-metallic minerals with a drastic reduction of the greenhouse gasses for
452 mass production industries.

453

454 **5. ACKNOWLEDGEMENTS**

455 The authors express their thanks to the project MAT-2017-86450-C4-1-R for the
456 financial support.

457

458

459 **6. REFERENCES**

460 [Agrawal, 1998](#)

461 D. K. Agrawal. Microwave processing of ceramics

462 Curr. Opin. Solid State Mater. Sci., 3 (1998), pp. 480-485.

463 [https://doi.org/10.1016/S1359-0286\(98\)80011-9](https://doi.org/10.1016/S1359-0286(98)80011-9)

464 [Bhattacharya and Basak, 2017](#)

465 M. Bhattacharya, T. Basak. Susceptor-Assisted Enhanced Microwave Processing of
466 Ceramics - A Review.

467 Crit. Rev. Solid State Mater. Sci. 42, 6 (2017), pp. 433–469.

468 <https://doi.org/10.1080/10408436.2016.1192987>

469 [Bindra and Bahel, 2010](#)

470 S. Bindra, S. Bahel. Low loss dielectric ceramics for microwaves applications: a review.

471 J. Ceram. Process. Res., 11, 3 (2010), pp. 316-321.

472 [Brindley and Nakahira, 1959](#)

473 G. W. Brindley, M. Nakahira. The Kaolinite-mullite reaction series: II, metakaolin.

474 J. Am. Ceram. Soc., 42, 7 (1959), pp. 314-318

475 <https://doi.org/10.1111/j.1151-2916.1959.tb14315.x>

476 [Catalá et al. 2015](#)

477 Jose M. Catala-Civera, Antoni J. Canós-Marín, Pedro Plaza-González, José D.

478 Gutiérrez Cano, Beatriz García Baños and Felipe L. Penaranda-Foix. Dynamic

479 Measurement of Dielectric Properties of Materials at High Temperature During

480 Microwave Heating in a Dual Mode Cylindrical Cavity.

481 IEEE Trans. on Microw. Theory and Techn. 63 (2015), pp. 2905-2914

482 [Chen et al., 2015](#)

483 J. C. H. J. Chen, Y. Sato, R. Kosaka, M. Hashisaka, K. Muraki, T. Fujisawa. Enhanced
484 electron-phonon coupling for a semiconductor charge quit in a surface phonon cavity.
485 Sci. Rep. 5 (2015), pp. 15176.

486 <https://doi.org/10.1038/srep15176>.

487 [Clark and Sutton, 1996](#)

488 D. E. Clark, W. H. Sutton. Microwave processing of materials.

489 Annu. Rev. Mater. Sci., 26 (1996), pp. 299-311.

490 <https://doi.org/10.1146/annurev.ms.26.080196.001503>

491 [Clark et al, 2005](#)

492 D. E. Clark, D.C. Folz, C. E. Folgar, M. M. Mahmoud. Microwave solutions for ceramic
493 engineers.

494 Published by the Am. Ceram. Soc., Westerville, OH, USA (2005), pp. 205–228.

495 ISBN: 978-1-574-98224-4

496 [Daphne Project, 2012](#)

497 Daphne European Project. Project ID: 314636 (2012-2015)

498 https://cordis.europa.eu/result/rcn/184183_es.html

499 [Fang et al., 2009](#)

500 C. Y. Fang, C. A. Randal, M. T. Lanagan, D. K. Agrawal. Microwaves processing of
501 electroceramic materials and devices.

502 J. Electroceram., 22 (2009), pp. 125-130.

503 <https://doi.org/10.1007/s10832-008-9441-2>

504 [Fernandez et al., 2015](#)

505 J. Fernández, E. Reyes-Davo, R. Reyes-Cánovas, J. García, E. Vela, A. Jara. Célula
506 calefactora, calefactor que hace uso de la misma, sistema de calefacción y uso del
507 mismo.

508 PCT ES2015/070712 and WO2016051003A1

509 [Ferrus et al., 2014](#)
510 T. Ferrus, A. Rossi, A. Andreev, T. Kodera, T. Kambara, W. Lin, S. Oda, D. A.
511 Williams. GHz photon-activated hopping between localized.
512 New J. Phys., 16 (2014), pp. 013016.
513 <https://doi.org/10.1088/1367-2630/16/1/013016>

514 [García-Baños et al., 2016](#)
515 B. García-Baños, J. M. Catalá Civera, F. L. Peñaranda-Foix, P. Plaza-González, G.
516 Llorens-Vallés. In situ monitoring of microwave processing of materials at high
517 temperatures through dielectric properties measurement.
518 Materials., 9 (2016), pp. 349.
519 <https://doi.org/10.3390/ma9050349>

520 [García-Baños et al., 2015](#)
521 B. Garcia-Baños, J. J. Reinoso, J. F. Fernández, P. J. Plaza-González, Dielectric
522 properties of ceramic frits up to 1200°C and correlation with thermal analyses.
523 AMPERE 2015 - 15th International Conference on Microwave and High Frequency
524 Heating. pp.108

525 [Giesse and Datta, 1973](#)
526 R. F. Giese, P. Datta. Hydroxyl orientation in Kaolinite, Dickite and Nacrite.
527 Am. Mineral., 58 (1973), pp. 471-479

528 [Hu and Liu, 2013](#)
529 Y. Hu, X. Liu. Chemical composition and surface properties of kaolins.
530 Miner. Eng. 16 (11) (2003), pp. 1279-1284.
531 <https://doi.org/10.1016/j.mineng.2003.07.006>

532 [Leonelli et al., 2008](#)
533 C. Leonelli, P. Veronesi, L. Denti, A. Gatto, L. Luliano. Microwaves assisted sintering of
534 green metal parts.

535 J. Mater. Process. Technol., 205 (2008), pp. 489-496.
536 <https://doi.org/10.1016/j.jmatprotec.2007.11.263>

537 [Lorite et al., 2012](#)

538 I. Lorite, M. S. Martín-González, J. J. Romero, M. A. García, J.L.G. Fierro, J. F.
539 Fernández. Electrostatic charge dependence on surface hydroxylation for different
540 Al₂O₃ powders.
541 Ceram. Int., 28 (2012), pp. 1427-1434.
542 <https://doi.org/10.1016/j.ceramint.2011.09.024>

543 [Mandal and Sen, 2017](#)

544 A. K. Mandal, R. Sen. An overview on microwave processing of material: A special
545 emphasis on glass melting.
546 Mater. Manuf. Processes., 32 1 (2017), pp. 1-20
547 <https://doi.org/10.1080/10426914.2016.1151046>

548 [Michot et al., 2008](#)

549 A. Michot, D. S. Smith, S. Degot, C. Gault. Thermal conductivity and specific heat of
550 Kaolinite: evolution with thermal treatment.
551 J. Eu. Ceram. Soc., 28 (2008), pp. 2639-2644.
552 <https://doi.org/10.1016/j.jeurceramsoc.2008.04.007>

553 [Oghbaei and Mirzaee, 2010](#)

554 M. Oghbaei, O. Mirzaee. Microwave versus conventional sintering: A review of
555 fundamentals, advantages and applications.
556 J. Alloys Comp., 494 (2010) pp. 175–189.
557 <https://doi.org/10.1016/j.jallcom.2010.01.068>

558 [Olivier et al., 2014](#)

559 J.G.J. Olivier, G. Janssens-Maenhout, M. Muntean, J.A.H.W. Peters. Trends in global
560 CO₂ emissions: 2014 Report. PBL Netherlands Environmental Assessment Agency.
561 The Hague, 2014.

562 [Ondruška et al., 2015](#)

563 J. Ondruška, V. Trnovcová, I. Štubna, R. Podoba, DC conductivity of ceramics with
564 calcite waste in the temperature range 20 - 1050°C
565 Ceramics - Silikaty 59, 2 (2015) 176-180.

566 [Ribeiro et al., 2004](#)

567 M. J. Ribeiro a, J. C. C. Abrantes a, J. M. Ferreira b, J. A. Labrincha. Predicting
568 processing-sintering-related properties of mullite–alumina ceramic bodies based on Al-
569 rich anodising sludge by impedance spectroscopy.
570 J. Eu. Ceram. Soc., 24 (2004), pp. 3841–3848.
571 <https://doi.org/10.1016/j.jeurceramsoc.2003.12.026>

572 [Roy et al., 1999](#)

573 R. Roy, D. Agrawal, J. P. Chen, S. Gedevarishvili. Full sintering of powdered-metal
574 bodies in a microwave field.
575 Nature., 399, 6737 (1999), pp. 668-670.
576 <https://doi.org/10.1038/21390>

577 [Roy et al, 2002](#)

578 R. Roy, R. Peelamedu, L. Hurtt, J. Cheng, D. Agrawal, Definitive experimental
579 evidence for microwave effects: radically new effects of separated E and H fields , such
580 as decrystallization of oxides in seconds.
581 Mater. Res. Innovations., 6, 3 (2002), pp. 128–140.
582 <http://dx.doi.org/10.1007/s10019-002-0199-x>

583 [Sperinck et al., 2011](#)

584 S. Sperinck, P. Raiteri, N. Marks, K. Wright. Dehydroxylation of Kaolinite to metakaolin-
585 a molecular dynamics study.
586 J. Mater. Chem. 21 (2011), pp. 2118-2125.
587 <https://doi.org/10.1039/c0jm01748e>

588 [Sahnoune et al., 2007](#)
589 F. Sahnoune, M. Heraiz, H. Belhouchet, N. Saheb and D. Redaoui, Thermal
590 Decomposition Kinetics of Algerian Tamazarte Kaolin by Differential Thermal Analysis
591 (DTA).
592 Acta Phys. Pol. A., 131 (3) (2007), pp. 382-385.
593 <https://doi.org/10.12693/APhysPolA.131.382>

594 [Sun et al., 2016](#)
595 J. Sun, W. Wang, Q. Yue. Review on Microwave-Matter Interaction: Fundamentals and
596 Efficient Microwave-Associated Heating Strategies.
597 Materials., 9 (2016), pp. 231.
598 <https://doi.org/10.3390/ma9040231>

599 [Tari et al., 1999](#)
600 G. Tari, L. Bobos, C. S. F. Gomes, J. M. F. Ferreira. Modification of Surface Charge
601 Properties during Kaolinite to Halloysite-7Å Transformation.
602 J. Colloid Interface Sci., 210 (1999), pp. 360–366.
603 <https://doi.org/10.1006/jcis.1998.5917>

604 [Thostenson and Chou, 1999](#)
605 E. T. Thostenson, T. W. Chou. Microwave processing: fundamentals and applications.
606 Composites Part A - App. Sci. Manufacturing., 30, 9 (1999) 1055-1071.
607 [https://doi.org/10.1016/S1359-835X\(99\)00020-2](https://doi.org/10.1016/S1359-835X(99)00020-2)

608 [Vaidhyanathan et al., 2001](#)

609 B. Vaidhyanathan, A.P. Singh, D.K. Agrawal, T.R. ShROUT, R. Roy, S. Ganguly,
610 Microwave Effects in Lead Zirconium Titanate Synthesis: Enhanced Kinetics and
611 Changed Mechanisms.

612 J. Am. Ceram. Soc. 84, 6 (2001), pp. 1197–1202.

613 <https://doi.org/10.1111/j.1151-2916.2001.tb00816.x>

614 [Varga, 2007](#)

615 G. Varga. The structure of Kaolinite and metakaolin.

616 Epitoayang., 2 (2007), pp. 6-9.

617 <http://dx.doi.org/10.14382/epitoanyag-jsbcm.2007.2>

618 [Zemanova et al. 2006](#)

619 M. Zemanová, G. Link, S. Takayama, R. Nüesch, M. Janek. Modification of layer
620 charge in smectites by microwaves.

621 Applied Clay Science 32 (2006) 271-282.

622 <https://doi.org/10.1016/j.clay.2006.01.002>

623 [Zhang et al., 2014](#)

624 Z. Zhang, X. Qiao, J. Yu. Microwave selective heating-enhanced reaction rates for
625 mullite preparation from kaolinite.

626 RSC Advances 4 (2014) 2640-2647.

627 <https://doi.org/10.1039/c3ra43767a>

628

629

630

631

632

633

634

635

636

637 **SUPPLEMENTARY INFORMATION**

638



639

640 *Supplementary Information 1.- Microwaves energy laboratory equipment.*

641

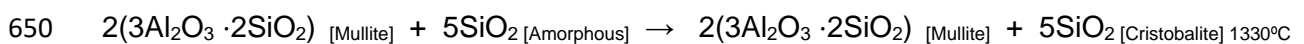
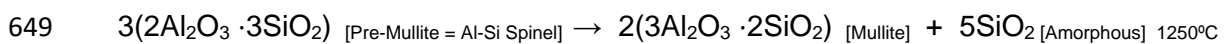
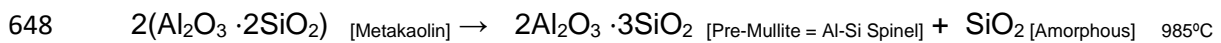
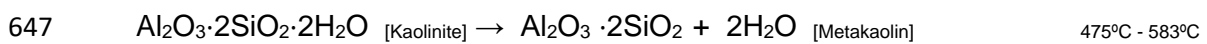
642

643

644

645

646



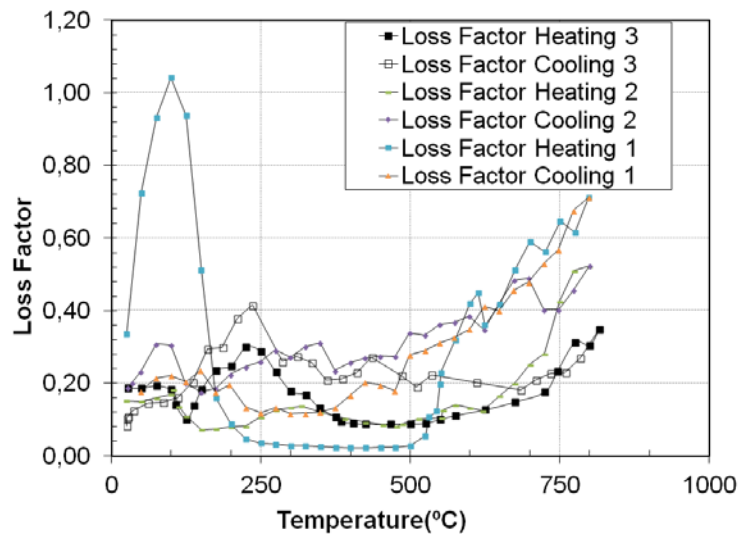
651

652

652 *Supplementary Information 2.- Processes with temperature form kaolin.*

653

654



655

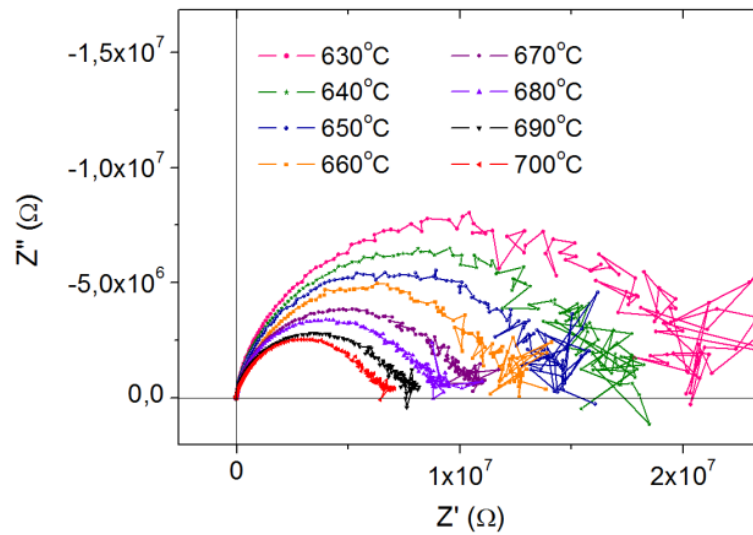
656 *Supplementary Information 3.- Dielectric properties (loss factor) of metakaolin during several heating-*
657 *cooling cycles. This time, temperature achieves only 800°C in order to not to crystallize mullite phase.*

658

659

660

661

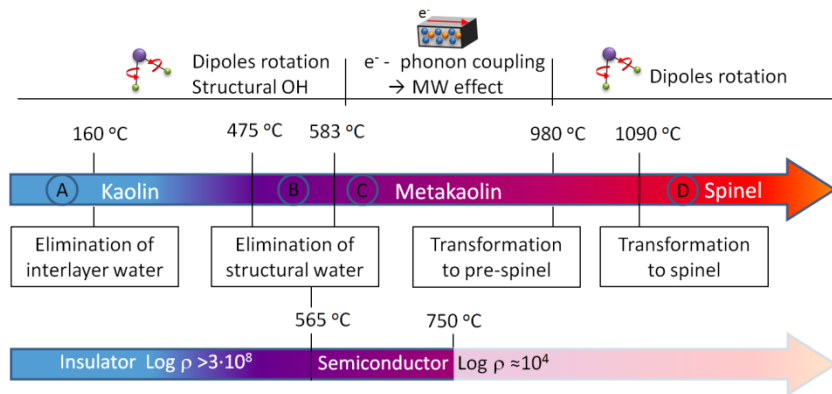


662

663 *Supplementary Information 4.- Impedance arcs of metakaolin sample (from kaolin clay heated at $T > 550^\circ\text{C}$)*
664 *at the temperature range $630^\circ\text{C} < T < 700^\circ\text{C}$, during heating process.*

665

666



668

669 Supplementary information 5.- Summary of processes in kaolin and later phases with
 670 temperature, dielectric behavior and causes of the heating.

671 (A) At the region A, from RT up to ~475°C, the dipole rotation is in the origin of the
 672 microwave heating of the kaolin. As the absorption of microwave is low, higher bandwidth and
 673 low heating rate are produced. In this region A, the presence of hydroxyl groups and the
 674 ionization of water occur on the crystal surfaces.

675 (B) At the range of temperature 475°C-583°C, the dehydroxylation of structural water into
 676 kaolinite takes place as it was observed by Tg study and the accommodation of the structure
 677 occurs up to ~650°C as it was demonstrated by DTA. During the process (at ~565°C), electrical
 678 measurements showed that DC resistivity of the sample decreases.

679 (C) From ~650°C and up to T~980°C, a high heating rate is observed when microwaves
 680 energy is applied to the sample. The high heating rate may be related to a Microwaves effect
 681 and it occurs as a consequence of the appearance of surface carriers originated from the
 682 uncompensated removal of hydroxyl groups from the crystal lattice. Carriers are activated by
 683 microwave absorption and the excess of energy is transmitted to the crystal lattice in term of
 684 electron-phonon coupling.

685 (D) Finally the charges as the mass transport occurs, the surface of the metakaolin reduces
 686 and at region D, from 980°C the heating curve decreases. At high temperature, the pre-spinel

687 phase is achieved and the atoms network is relaxed and dilated, the systems has higher amount
688 of vibration energy and the dipoles rotation is favored.